Gut Bacteria Composition Drives Primary Resistance to Cancer Immunotherapy in Renal Cell Carcinoma Patients

Lisa Derosa [a,b,c,d,†,*], *Bertrand Routy* [e,f,†], *Marine Fidelle* [a,b,c,g,h,†], *Valerio Iebba* [a,b], *Laurie Alla* [i], *Edoardo Pasolli* [j], *Nicola Segata* [k,l], *Aude Desnoyer* [a,h,m], *Filippo Pietrantonio* [n], *Gladys Ferrere* [a,b], *Jean-Eudes Fahrner* [a,b,c,o], *Emmanuelle Le Chatellier* [i], *Nicolas Pons* [i], *Nathalie Galleron* [i], *Hugo Roume* [i], *Connie P.M. Duong* [a,b], *Laura Mondragón* [c,p,q], *Kristina Iribarren* [r], *Mélodie Bonvalet* [a,b], *Safae Terrisse* [a,b,c,d], *Conrad Rauber* [a,b,c], *Anne-Gaëlle Goubet* [a,b,c], *Romain Daillère* [r], *Fabien Lemaitre* [r], *Anna Reni* [a,b], *Beatrice Casu* [a,b], *Maryam Tidjani Alou* [a,b], *Carolina Alves Costa Silva* [a,b], *Didier Raoult* [s], *Karim Fizazi* [a,d], *Bernard Escudier* [a,d], *Guido Kroemer* [p,q,r,s,t,u,v], *Laurence Albiges* [a,c,d,†], *Laurence Zitvogel* [a,b,c,d,g,r,u,†,*]

[a] *Gustave Roussy Cancer Campus (GRCC), Villejuif, France;* [b] *Institut National de la Santé et de la Recherche Médicale (INSERM) U1015, Équipe Labellisée—Ligue Nationale contre le Cancer, Villejuif, France;* [c] *Faculté de Médecine Kremlin-Bicêtre, Université Paris Sud, Université Paris Saclay, France;* [d] *Department of Medical Oncology, Gustave Roussy Cancer Campus (GRCC), Villejuif, France;* [e] *Hematology-Oncology Division, Department of Medicine, Centre Hospitalier de l'Université de Montréal (CHUM), Montréal, QC, Canada;* [f] *Centre de Recherche du Centre Hospitalier de l'Université de Montréal (CRCHUM), Montréal l, Canada CHUM, Montréal, QC, Canada;* [g] *Center of Clinical Investigations in Biotherapies of Cancer (CICBT) 1428, Villejuif, France;* [h] *Faculté de Pharmacie, University Paris-Saclay, Chatenay-Malabry, France;* [i] *Université Paris-Saclay, INRAE MetaGenoPolis, Jouy-en-Josas, France;* [j] *Department of Agricultural Sciences, University of Naples Federico II, Napoli, Italy;* [k] *Department CIBIO, University of Trento, Trento, Italy;* [l] *Istituto Europeo di Oncologie, Milan, Italy;* [m] *Gustave Roussy Cancer Campus, Laboratory of Immunomonitoring in Oncology, CNRS-UMS 3655 and INSERM-US23, Villejuif, France;* [n] *IRCCS Istituto Nazionale dei Tumori Foundation, Milan, Italy;* [o] *Transgene S.A., Illkirch-Graffenstaden, France;* [p] *Cell Biology and Metabolomics Platforms, Gustave Roussy Cancer Campus, Villejuif, France;* [q] *Equipe labellisée par la Ligue contre le cancer, Université de Paris, Sorbonne Université, INSERM U1138, Centre de Recherche des Cordeliers, Paris, France;* [r] *EverImmune, GRCC, Villejuif, France;* [s] *Aix-Marseille Université, MEPHI, IRD, IHU Méditerranée Infection, Marseille, France;* [t] *Pôle de Biologie, Hôpital Européen Georges Pompidou, AP-HP, Paris, France;* [u] *Suzhou Institute for Systems Medicine, Chinese Academy of Medical Sciences, Suzhou, China;* [v] *Department of Women's and Children's Health, Karolinska Institute, Karolinska University Hospital, Stockholm, Sweden*

Article info

Article history:
Accepted April 20, 2020

Associate Editor:
Maarten Albersen

Abstract

Background: The development of immune checkpoint blockade (ICB) has revolutionized the clinical outcome of renal cell carcinoma (RCC). Nevertheless, improvement of durability and prediction of responses remain unmet medical needs. While it has been recognized that antibiotics (ATBs) decrease the clinical activity of ICB across various malignancies, little is known about the direct impact of distinct intestinal nonpathogenic bacteria (commensals) on therapeutic outcomes of ICB in RCC.
Objective: To evaluate the predictive value of stool bacteria composition for ICB efficacy in a cohort of advanced RCC patients.
Design, setting, and participants: We prospectively collected fecal samples from 69 advanced RCC patients treated with nivolumab and enrolled in the GETUG-AFU 26 NIVO-

† These co-first and -last authors contributed equally to this work.
* Corresponding authors. Gustave Roussy Cancer Center, 114 rue Edouard Vaillant, 94805 Villejuif Cedex, France. Tel. +33 69850 8955 (L. Derosa). Tel. +33 14211 5041; Fax: +33 14211 6094 (L. Zitvogel).
E-mail addresses: deros.lisa@gmail.com, Lisa.DEROSA@gustaveroussy.fr (L. Derosa), laurence.zitvogel@gustaveroussy.fr (L. Zitvogel).

Keywords:
Kidney cancer
Renal cell carcinoma
Microbiota
Nivolumab
Antibiotics
Tyrosine kinase inhibitor
Immune checkpoint inhibitor

REN microbiota translational substudy phase 2 trial (NCT03013335) at Gustave Roussy. We recorded patient characteristics including ATB use, prior systemic therapies, and response criteria. We analyzed 2994 samples of feces from healthy volunteers (HVs). In parallel, preclinical studies performed in RCC-bearing mice that received fecal transplant (FMT) from RCC patients resistant to ICB (NR-FMT) allowed us to draw a cause-effect relationship between gut bacteria composition and clinical outcomes for ICB. The influence of tyrosine kinase inhibitors (TKIs) taken before starting nivolumab on the microbiota composition has also been assessed.
Outcome measurements and statistical analysis: Metagenomic data (MG) from whole genome sequencing (WGS) were analyzed by multivariate and pairwise comparisons/fold ratio to identify bacterial fingerprints related to ATB or prior TKI exposure and patients' therapeutic response (overall response and progression-free survival), and compared with the data from cancer-free donors.
Results and limitations: Recent ATB use ($n = 11$; 16%) reduced objective response rates (from 28% to 9%, $p < 0.03$) and markedly affected the composition of the microbiota, facilitating the dominance of distinct species such as *Clostridium hathewayi*, which were also preferentially over-represented in stools from RCC patients compared with HVs. Importantly, TKIs taken prior to nivolumab had implications in shifting the microbiota composition. To establish a cause-effect relationship between gut bacteria composition and ICB efficacy, NR-FMT mice were successfully compensated with either FMT from responding RCC patients or beneficial commensals identified by WGS-MG (*Akkermansia muciniphila and Bacteroides salyersiae*).
Conclusions: The composition of the microbiota is influenced by TKIs and ATBs, and impacts the success of immunotherapy. Future studies will help sharpen the role of these specific bacteria and their potential as new biomarkers.
Patient summary: We used quantitative shotgun DNA sequencing of fecal microbes as well as preclinical models of fecal or bacterial transfer to study the association between stool composition and (pre)clinical outcome to immune checkpoint blockade. Novel insights into the pathophysiological relevance of intestinal dysbiosis in the prognosis of kidney cancer may lead to innovative therapeutic solutions, such as supplementation with probiotics to prevent primary resistance to therapy.

1. Introduction

Metastatic renal cell carcinoma (RCC) has long been considered an "immunogenic malignancy" susceptible to different immunotherapies [1–3]. In this tumor type, the prognostic role of the immune contexture was broadly heralded. In both primary and metastatic RCC, CD38+ tumor-associated macrophages, immature dendritic cells, absence of tertiary lymphoid organs or overt expression of T-cell inhibitory receptors, and tumoral programmed death ligand 1 (PD-L1) are associated with shorter overall survival (OS) in both primary and metastatic RCC [4–9].

Despite the success seen with interleukin-2 [1,3], an immuno-oncological revolution has been truly precipitated by the regulatory approval of immune checkpoint blockers (ICBs), agents that release latent anticancer immunity. After positive trials in a second-line (2L) setting [10], Checkmate 214 study combining anti–PD-1 and anti–CTLA-4 in first-line (1L) metastatic RCC [11], as well as results from randomized phase 3 trials JAVELIN Renal 101, KEYNOTE-426, and IMmotion 151, provides evidence that anti–PD-(L)1–based combination therapy with anti–CTLA-4 or tyrosine kinase inhibitors (TKIs) has superior efficacy to standard care sunitinib [12–15]. In this rapidly expanding field, patient stratification is now required to predict tumor aggressiveness. Moreover, immune-related adverse events are common and lead to complex treatment paradigms. These obstacles can be overcome by exploring the impact of neoangiogenesis/hypoxia patterns and Th1 geared inflammatory profile to generate novel molecular classification of RCC [16,17]. In addition, several arguments are currently in favor of the influence of the intestinal microbiome in oncogenesis and response to therapy, with some establishing cause-effect relationships between the fecal composition and clinical outcome in mice and humans. First, distinct commensals exert protumorigenic effects, as observed in colon and pancreatic cancers [18]. Second, antibiotics (ATBs), the most common and significant cause of gut dysbiosis, compromise the efficacy of ICBs or combination ICBs (CICBs), independently of the tumor histology [19–21]. Third, microbiome profiling revealed different fingerprints between responders (Rs) and nonresponders (NRs) to ICBs across groups and countries [20,22,23]. Finally, certain immunostimulatory bacteria species (*Akkermansia muciniphila* [20], *Bifidobacterium longum* [23,24], and *Bacteroides fragilis* [25]) or strains (*Enterococcus hirae* 13144 but not 13344 [26]) can elicit systemic immune responses and reprogram the tumor microenvironment in mouse tumors treated with anti–CTLA-4 and/or anti–PD-1 antibodies.

In 2018, our team reported the predictive value of the metagenomic-based stool composition of a mixed cohort of non–small cell lung cancer (NSCLC; $n = 60$) and RCC ($n = 40$) patients at diagnosis [20] for progression-free survival (PFS) at 3 mo or best outcome to anti–PD-1 blockade. Here, we analyzed 69 metastatic RCC patients as a single and independent cohort and described the imprinting of ATBs and TKIs on microbial composition, identifying beneficial commensals circumventing resistance to ICBs in the avatar renal cell carcinoma (RENCA) murine model [20,27].

2. Patients and methods

A full description of materials and methods is available in the Supplementary material. Hereafter, only the general procedures are reported, especially taking into consideration the "guidelines for reporting of statistics for clinical research in urology" provided in the paper by Assel et al [28].

2.1. Patient characteristics and clinical study details

Inclusion criteria were patients with stage IV RCC and disease progression during or after one or more prior regimens, who received nivolumab intravenously (i.v.) 3 mg/kg every 2 wk until disease progression or intolerable toxicity in the NIVOREN GETUG-AFU 26 phase 2 trial (EudraCT: 2015-004117-24; NCT03013335) [29]. Computed tomography scans were performed at baseline and every 8–12 wk for the 1st year and then every 12–15 wk until disease progression. Tumor response was assessed using the Response Evaluation Criteria in Solid Tumors version 1.1 (RECIST v1.1; Fig. 1A) [30]. All patients were followed up until death or data lock (September 2018). From February 2016 to September 2018, a total of 85 patients with RCC were enrolled in the NIVOREN GETUG-AFU 26 phase 2 trial at Gustave Roussy. In the Microbiota translational substudy, we collected baseline (T0-T4) feces from 69 patients (Fig. 1A). Results from 40 patients were previously reported in a pooled analysis with 60 NSCLC patients [20]. Here, RCC have been analyzed for the first time as a single cohort after inclusion of additional patients. The demographic and clinical characteristics of the patients are illustrated in Supplementary Table 1.

2.2. Collection of samples

Feces were prospectively collected according to International Human Microbiome Standards guidelines (SOP_03_V1) [31] at different time points: before the first nivolumab injection (T0, <1 mo before), after the 2nd (T4, 4 wk), after the 4th (T8, 8 wk), and after the 12th (T24, 24 wk) injection (Fig. 1A). We reported that the microbiota did not change significantly within T0 and T4 [30]; T4 specimens were used as baseline when T0 samples were not available. Study name and ethics for this translational part of the trial was "Oncobiotics - B2M"; ethics protocol number was PP:15-013. All patients provided written informed consent that was based on the principles of the Declaration of Helsinki. Blood was prospectively collected before the first nivolumab injection. Study name and ethics for this translational part of the trial was "GETUG-AFU 26" UC-0160/1506.

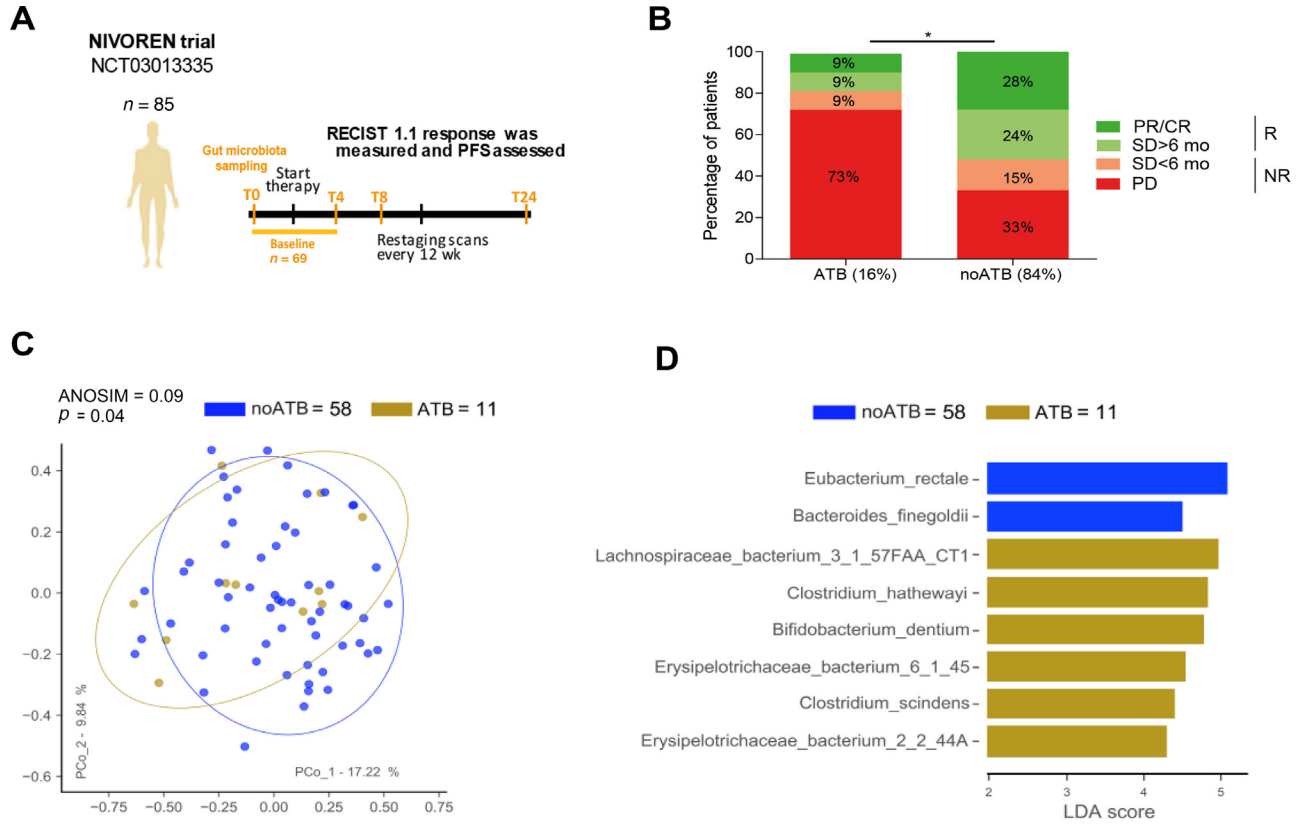

Fig. 1 – Antibiotics compromise the efficacy of PD-1 blockade and affect the intestinal composition of feces in advanced renal cell carcinoma patients. (A) Patients with advanced renal cell carcinoma ($n = 85$) were evaluated for clinical outcomes and correlative fecal microbiota ($n = 69$) analyses prior to and following initiation of anti–PD-1 blockade. Tumor response was assessed using the Response Evaluation Criteria in Solid Tumors version 1.1 (RECIST v1.1). (B) The best overall response was stratified by the use of ATBs (ATB group = 11, patients who took antibiotics within 2 mo of prior anti–PD-1 blockade; noATB group = 58, patients who did not take antibiotics). The p value was obtained with two-tailed chi-square test; Yates correction and significant p values are indicated with * (* $p < 0.05$, ** $p < 0.01$, *** $p < 0.001$). (C) Beta-diversity ordination plot based on principal coordinate analysis of normalized and standardized data of fecal microbiota composition in pretreatment (T0-T4) samples ($n = 69$). Bacterial relative abundances were obtained with MetaOmineR package developed in "R" by INRA. Percentage of variance embraced by each new coordinate is reported in percentages for each axis. Ellipses describing the 95% of confidence are even depicted for each cohort. ANOSIM metrics was implemented with 999 permutations to assess differences among ATB (gold) and noATB (blue) cohorts. (D) LEfSe graph was implemented in Python version 2.7 on bacterial species undergoing two-stage Benjamini-Hochberg false detection rate at 10%, resulting in the identification of the most discriminant species for each cohort based on LDA score.

ATB = antibiotic; CR = complete response; LDA = linear discriminant analysis; LEfSe = linear discriminant analysis of effect size; NR = nonresponder; PR = partial response; PD = progressive disease; PD-1 = programmed death 1; PFS = progression-free survival; R = responder; SD = stable disease.

2.3. Outcome measurements

Data regarding patient demographics and baseline characteristics including tumor/treatment details (any treatment prior to nivolumab) and recent ATB use (within 60 d of nivolumab) were collected (Supplementary Table 1). Outcome measures of interest were objective response rate (ORR), best overall response (BOR), and PFS. ORR was defined as the number of patients with a complete response and/or a partial response at any time based on RECIST. BOR was defined as the investigator-assessed best response (complete response, partial response, stable disease, or progressive disease) from the start date of nivolumab to the end of treatment (for objectively documented disease progression or subsequent therapy, whichever occurred first). PFS was defined as the time from the start date of nivolumab to first documented RECIST-defined tumor progression or death from any cause. All patients were followed up until death or data lock (September 2018). Patients were divided by the absence of progressive disease at 12 mo after initiation of ICBs in PFS >12 mo (those with the absence of progressive disease at 12 mo) or PFS <12 mo (who progressed in <12 months) and by BOR in Rs (those in complete response, partial response, or stable disease for >6 mo) and NRs (who progressed or were in stable disease for <6 mo or died) to nivolumab. Survival curves and corresponding p values (log-rank test) were generated with Prism5 (GraphPad).

2.4. Metagenomic and network analysis

Total DNA was extracted from stool specimens and sequenced with Ion-Proton technology following MetaGenoPolis (INRA) workflow [32,33]. Cleaning, filtering, and classification of reads were performed with two different pipelines: MetaOMineR and MetaPhlAn2 [34]. A full description of both DNA purification and metagenomic pipelines is available in the Supplementary material. Starting from abundance matrices, only taxa that were present in at least 20% of all samples were considered, and then raw data were normalized and standardized (Sci-Kit-learn version 0.20.3). Measurements of alpha-diversity (within sample diversity) such as observed_otus and Shannon index were calculated at species level (SciKit-Bio version 0.4.1). Exploratory analysis of beta-diversity (between sample diversity) was calculated using the Bray-Curtis measure of dissimilarity and represented in principal coordinate analyses (PCoA), while for hierarchical clustering analysis "Bray-Curtis" metrics and "complete linkage" methods were implemented [35].

2.5. Statistical analysis

Supervised partial least square discriminant analysis (PLS-DA) and the subsequent variable importance plot (VIP) were used to find out the most discriminant bacterial species among the cohorts in respect to BOR. Two-tailed Mann-Whitney U and Kruskal-Wallis tests were employed (SciPy version 1.3) to assess the significance of pairwise and multiple comparisons, respectively, considering a p value of ≤ 0.05. Cross-correlation Pearson matrices for network analysis (metric = Bray-Curtis, method = complete linkage) were generated and visualized with Gephi version 0.9.2. All p values underwent a Benjamini-Hochberg two-stage false detection rate (FDR) at 10% and were considered significant if ≤ 0.05.

2.6. Preclinical study details

Using a previously validated preclinical model, fecal microbiota transfer (FMT) using patient's stools was performed following 3 d of ATBs in BALB/c mice [20]. Two weeks later, luciferase engineered RENCA cells were orthotopically injected in the right kidney. Treatment began 7 d after tumor inoculation (day 7). Mice were randomized to receive intraperitoneally every 4 d anti–PD-1 monoclonal antibodies (mAbs) and anti–CTLA-4 mAbs (CICBs) with or without oral gavage of commensals/fecal samples from R patients or isotype control mAb. Tumor growth was monitored by weighing the kidneys at sacrifice and by a longitudinal follow-up of whole-body luminescence using IVIS Imaging System 50 Series (Analytic Jenap).

3. Results

3.1. ATBs compromise the efficacy of ICBs

Sixty-nine patients were included in this study during a median follow-up period of 23.54 mo (range 0.66–32.21 mo). Disease progression was observed in 61 patients, and 24 patients died. Among 69 patients included, 11 (16%) received ATBs. Baseline characteristics of patients in the ATB and noATB groups were not significantly different, excluding the number of prior treatments (Supplementary Tables 1A and 1B). Patients who received ATBs ($n = 11$, 16%) had a lower ORR than the noATB subgroup (9% vs 28%, $p < 0.03$; Fig. 1B) and lower PFS and OS (Supplementary Fig. 1). Based on prior studies demonstrating higher diversity of the gut microbiome in R melanoma patients to anti–PD-1 blockade [22], we first compared the median alpha-diversity in ATB versus noATB group, and observed no significant differences across multiple diversity metrics (Shannon or observed operational taxonomic units or Simpson index, not shown). We then performed PCoA for microbial beta-diversity, which provides a measure of the overall relatedness (or lack thereof) between samples. Significant differences separated bacterial species from feces of ATB versus noATB individuals (ANOSIM = 0.089; $p < 0.04$; Fig. 1C). Using linear discriminant analysis of effect size (LEfSe) [36], coupled to a pairwise comparison of relative taxonomic abundances (for species having a prevalence of $\geq$20%) within each level using bootstrapping of two-tailed Mann-Whitney U tests (with 1000 permutations and correction for continuity and ties), we concluded that selected bacterial taxa were over-represented in noATB stools such as *Eubacterium rectale* ($p = 0.02$), while others were over-represented in ATB fecal materials such as *Erysipelotrichaceae bacterium_2_2_44A* ($p = 0.02$) and *Clostridium hathewayi* ($p < 0.02$; Fig. 1D).

Altogether, we surmise that ATBs compromised the clinical efficacy of ICBs in RCC patients, and altered the taxonomic beta-diversity and composition of intestinal microbiota.

3.2. Intestinal microbiota composition predicts clinical outcome to ICBs in the cohort that did not take ATBs

Given the confounding factor of ATB uptake on microbiota composition, we firstly considered only no-ATB patients ($n = 58$). We started analyzing whether metagenomic profiles of baseline stools (T0-T4) could predict PFS (at 3, 6, 9, and 12 mo) or Rs versus NRs using BOR. The taxonomical annotation of each metagenomic species (MGS) was performed based on gene homology to previously sequenced organisms (using blastN against the nt and whole genomic sequencing (Meta-Hit) [32] as well as the MetaPhlAn database and pipeline [36]). Higher richness (alpha-diversity) of the samples evaluated both at the gene

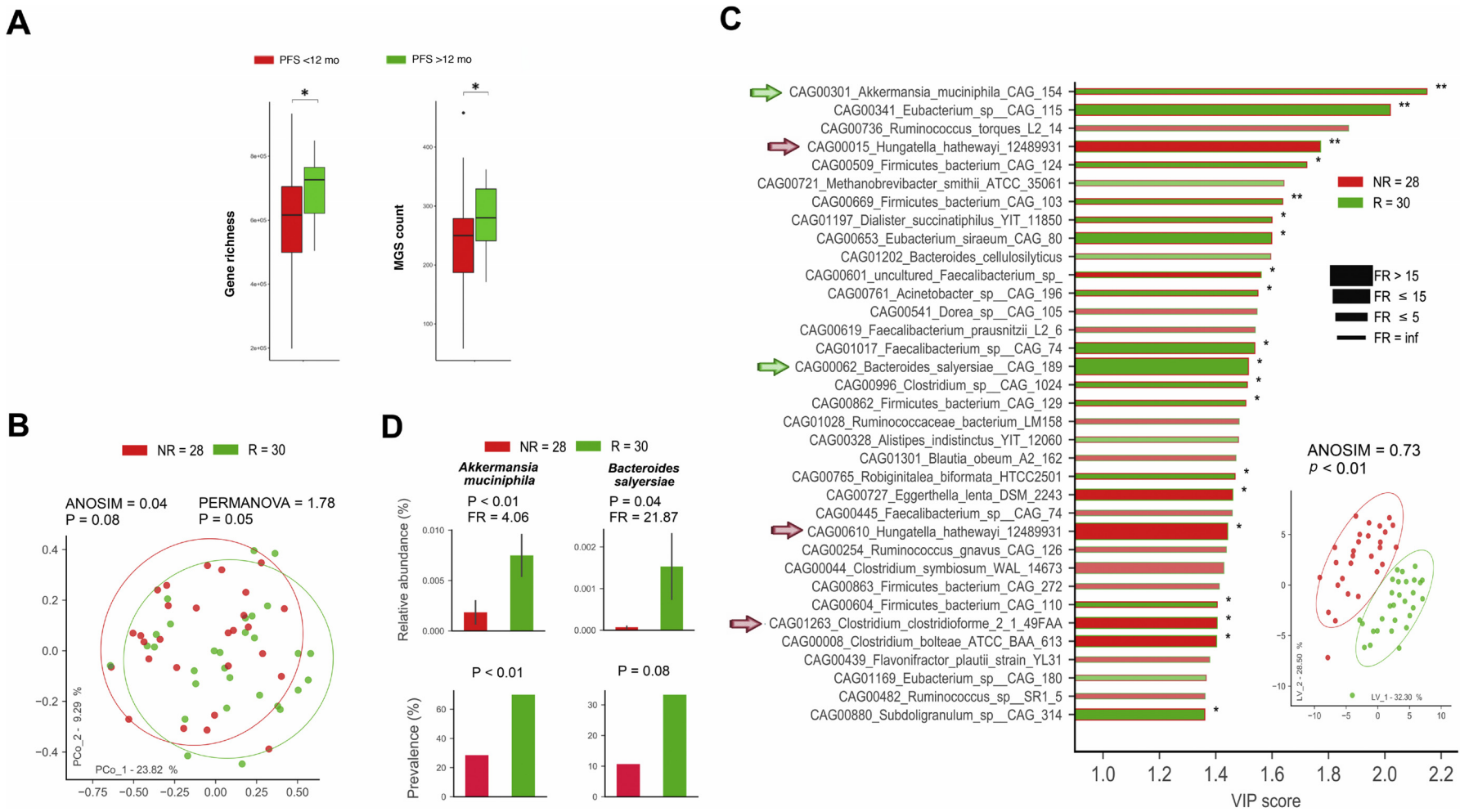

Fig. 2 – Metagenomic analyses (MetaOmineR pipeline) of fecal samples predict response of anti–PD-1 mAb in renal cell carcinoma patients. (A) Shotgun sequencing of fecal microbiota in noATB baseline (T0-T4) samples ($n = 58$) with representation of gene richness and MGS count for all cancer patients according to PFS at 12 mo. Mean ± SEM of count is depicted for patients who experienced PFS for >12 or <12 mo. (B) Beta-diversity ordination plot based on principal coordinate analysis of normalized and standardized data of fecal microbiota composition in noATB pretreatment (T0-T4) samples ($n = 58$). Bacterial relative abundances were obtained with MetaOmineR package developed in "R" by MetaGenoPolis. Percentage of variance embraced by each new coordinate is reported in percentages for each axis. Ellipses describing the 95% of confidence are even depicted for each cohort. ANOSIM and PERMANOVA metrics were implemented with 999 permutations to assess differences according to R (complete response or partial response or stable disease >6 mo, green) and NR (death or progressive disease or stable disease <6 mo, red). (C) Variable importance plot (VIP) was implemented within partial least square discriminant analysis (inset differentiating NR and R), describing the 35 most discriminant species in descending order of importance. Arrows are depicted to highlight species of importance. Each bar report the following information: (1) length, VIP score; (2) bar color, cohort in which the species has the highest mean relative abundance (high); (3) edge color, cohort in which the species has the lowest mean relative abundance (low); (4) thickness, fold ratio (FR) among high and low; and (5) significance of Mann-Whitney *U* test among high and low (* $p < 0.05$, ** $p < 0.01$, *** $p < 0.001$). (D) Bar plots of relative abundances (within the 0–1 interval) and prevalence of selected species (*A. muciniphila* and *B. salyersiae*). The *p* values for relative abundances were obtained after two-tailed Mann-Whitney *U* test, while *p* values for prevalence were retrieved by chi-square test.

ATB = antibiotic; mAb = monoclonal antibody; MGS = metagenomic species; NR = nonresponder; PD-1 = programmed death 1; PFS = progression-free survival; R = responder; SEM = standard error of the mean.

richness count (GC) or MGS levels correlated with the clinical response defined by the absence of PD at 12 mo after initiation of ICBs (Fig. 2A).

Then, we performed the PCoA (beta-diversity) using a threshold of bacteria prevalence of ≥20%. When segregating R from NR (according to BOR), we observed a significant separation among the two groups (Fig. 2B), with over-representation of distinct species including *A. muciniphila* ($p < 0.02$), *Bacteroides salyersiae* ($p = 0.04$), *and Eubacterium siraeum* ($p = 0.01$), and a trend toward *Clostridium ramosum* (ns) and *Alistipes senegalensis* (ns) in the R group, using both the MetaPhlAn2 (Supplementary Fig. 2) and the MetaOMiner pipelines (Fig. C), and of *E. bacterium_2_2_44A* ($p < 0.01$), *C. hathewayi* ($p < 0.01$), and *Clostridium clostridioforme* in the NR group (ANOSIM = 0.727; $p < 0.0009$, Fig. 2C), as observed with ATB uptake (Fig. 1D). Both the prevalence and the relative abundance of *A. muciniphila* and *B. salyersiae* were higher in Rs versus NRs in RCC patients' stools, using either one of these catalogs (Fig. 2D and Supplementary Fig. 2C). Of note, according to the nomenclature taxonomy, *C. hathewayi* is the same bacterium species as *Hungatella hathewayi* [37].

Considering higher GC and MGS counts at baseline in patients with PFS longer than 12 mo and almost significant beta-diversity between Rs and NRs (BOR; Fig. 2A and 2B), we addressed whether paired metagenomic profiles could change over time under ICB therapy by performing a longitudinal analysis of stools (T0, T4, T8, and T12) correlating with BOR or PFS at 12 mo. When excluding ATB usage ($n = 58$), MGS count was significantly higher in R patients than in NR patients at T0 and T4 (Supplementary Fig. 3A, left). Similarly, MGS count was significantly higher in patients with PFS longer than 12 mo than in those with PFS shorter than 12 mo at T0 and T8 (Supplementary Fig. 3B, left). Interestingly, we observed higher GC only in patients with PFS longer than 12 mo compared with those with PFS shorter than 12 mo at T0 and T8 (Supplementary Fig. 3B, left).

Finally, to perform a robustness test across at least three clinical parameters (BOR, PFS3, PFS6, PFS9, PFS12), we took into consideration all 69 individuals and found 27 reliable MGS (out of 1347) contrasting R ($n = 21$) and NR ($n = 6$) patients (based on the cliff delta for each MGS recovered in >50% tests). Among these selected MGS, four were in common with NSCLC microbiome profiles (listed in Supplementary Table 2) [20], especially encompassing *A. muciniphila* associated with favorable outcome during anti–PD-1 blockade. Of note, the robustness of MGS for the prediction was superior in long-term clinical readouts (not shown).

Altogether, we conclude that the alpha- and beta-diversity of stool composition could be used to stratify the RCC patient population in R and NR individuals and to predict patients with PFS longer than 12 mo.

3.3. RCC-associated gut dysbiosis fingerprint

Given the commonalities observed between MGS resulting from ATB-induced dysbiosis and species associated with primary resistance (NR) to immunotherapy, and assuming that NR patients harbor a "dysbiotic" fecal composition, we analyzed MGS discriminating RCC cancer patients from control adults (healthy volunteers [HVs], $n = 2994$; description in the Supplementary material). Significant differences in stool composition were observed between RCC patients and HVs (PCoA not shown, $p < 0.001$; LEfSe; Supplementary Fig. 5). Hence, by merging only significant species in each intersection (ATB, yes/no; RCC, yes/no; NR, yes/no), we found only two distinct species shared between the fecal repertoires of diseased groups (ATB, yes; RCC, yes; NR, yes), that is, *C. hathewayi* and *C. clostridioforme*. Conversely, no common species were shared between the opposite groups. Interestingly, *A. senegalensis* and *C. ramosum* were the only two common spp. between R and "noATB" subgroups, while *Dorea longicatena, Dorea formicigenerans, E. rectale*, and *Streptococcus salivarius* were all shared between HVs and "noATB" cancer patients (Supplementary Tables 3 and 4, and Supplementary Fig. 5).

To further study the links between these commensals relevant in RCC patients with the peripheral immune tonus, we performed Pearson correlations on normalized and standardized data between activation and exhaustion markers on blood $CD4^+$ and $CD8^+$ T lymphocytes (assessed in flow cytometry analyses at baseline) and the relative abundance of these commensals. Indeed, we found positive correlations between *D. formicigenerans* and $CD8^+CD69^+$ T cells (only in R patients, not shown) as well as negative associations between *C. clostridioforme* and CD137/4.1BB expressing $CD4^+$ T lymphocytes and memory CXCR5-CCR6-CCR4-CCR10-$CXCR3^+CD8^+$ T cells (Tc1; Supplementary Fig. 6), supporting the potential link of these species with the immune system.

3.4. Prior TKI and ATB uses are associated with distinct gut microbiota "guilds" in RCC patients

The majority of RCC patients ($n = 47$, 68%) received one previous line of TKIs before starting nivolumab (Supplementary Table 1). Sunitinib ($n = 49$, 71%) or axitinib ($n = 13$, 19%) were the most frequently administered TKIs. Co-occurrence network analysis revealed six "species interaction groups" referred to as "SIGs" [38], highlighting that (1) ATBs and axitinib were the most powerful medications shifting fecal microbiota (using cross-validation model, predictive power for ATBs = 84%, for axitinib = 81%, and for sunitinib = 69%), and (2) defined bacterial species drove the stratification of the whole RCC network into "SIGs", such as *A. muciniphila* for Rs and *D. formicigenerans* for noATB patients (random forest analysis; Supplementary Fig. 4).

3.5. Oral gavage with immunostimulatory or beneficial commensals or feces from responding RCC patients rescues primary resistance in RCC tumor-bearing mice

To further provide evidence of a cause-effect relationship between microbiota composition and therapy outcome, we humanized BALB/c mice gut microbiota sterilized by ATBs with RCC patient stools 15 d prior to orthotopic inoculation of luciferase engineered RENCA. Transfer of 15 human stool

specimens (five R and 10 NR patients, all no ATB users) by oral gavage (referred to "FMT" henceforth) in ATB-treated avatar mice that were subsequently implanted with RENCA-induced significant responses (when mice received FMT from R human donors) or resistance (when mice received FMT from NR human donors) to ICBs. It should be noted that we observed 27% of exceptions of concordance between patient's response and mouse recipient's response to ICBs: only four stool specimens above 15 FMT were used (Supplementary Table 5, and Fig. 3A and 3B). However, compensation of NR-FMT (that did not contain *A. muciniphila* or *B. salyersiae*) with oral administration of immunostimulatory *A. muciniphila* or *B. salyersiae* or R-FMT prior to each ICB cycle restored sensitivity to therapy (kidney weight at sacrifice [Fig. 3D] and decreased luminescence [Fig. 3C and 3E]). Despite strong co-occurrence of *B. salyersiae* with other commensal species (Supplementary Fig. 4A and 4B) varying in their identity in the R versus NR networks (Supplementary Fig. 4C), the antitumor efficacy of the former bacterium was not boosted by coadministration of a neighboring species (Supplementary Fig. 7C).

In conclusion, bacteria contrasting R and NR in our 69 RCC cohort compensate the lack of responsiveness observed with NR-FMT in avatar mice, establishing a cause-effect relationship between favorable bacterial composition of feces and clinical outcome.

3.6. *Antiangiogenic TKIs induce an intestinal microbiota shift*

Data from the co-occurrence network analysis revealed "SIGs" (Supplementary Fig. 4). Interestingly, axitinib (similar to ATBs) appeared to influence SIG distribution markedly within network topology (RF importance), more specifically SIG2, centered by *Odoribacter splanchnicus*, belonging to the same community as *D. longicatena* (Supplementary Fig. 4). To assess the distinct bacteria related to TKIs, we compared a subgroup of patients who had taken TKIs in 1L (within our 69 RCC patients' stools, regardless of ATBs) with HVs. Over-

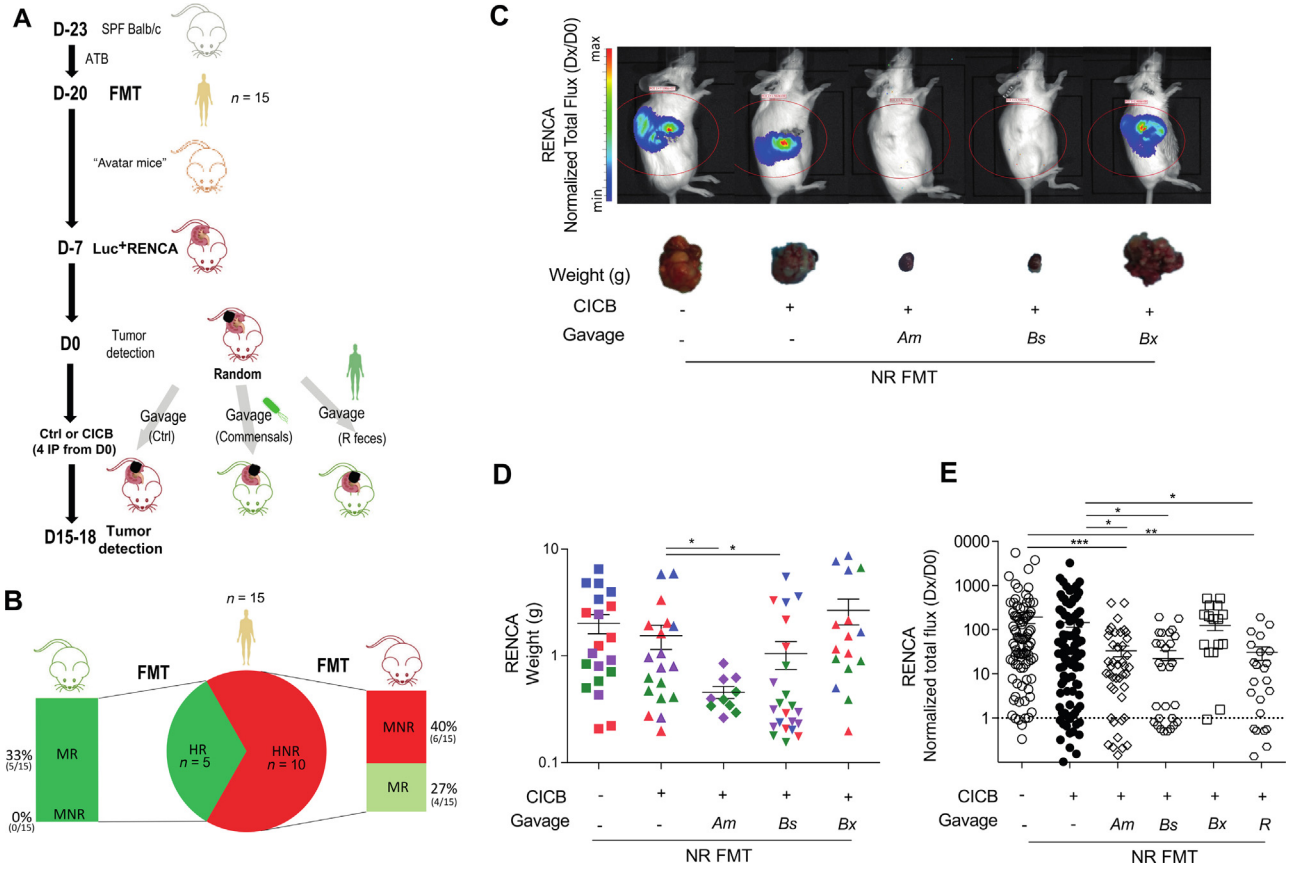

Fig. 3 – Oral gavage with immunostimulatory commensals or feces from responder RCC patients rescues the primary resistance in RCC tumor-bearing mice. (A) Experimental setting: fecal microbial transplantation (FMT) was performed following 3 d of ATB in specific pathogen-free (SPF) BALB/c mice. Two weeks later, luciferase engineered renal cell carcinoma (Luc$^+$RENCA) were orthotopically inoculated and anti–PD-1 plus anti–CTLA-4 mAb (CICB) or isotype control mAb (Ctrl) were inoculated intraperitoneally every 4 d starting from day 7. In addition, on day 4, oral administration of commensals *A. muciniphila* (*Am*), *B. salyersiae* (*Bs*), bacteria *B. xylanosolvens* (*Bx*), or feces from responder patients (R) to recipient mice receiving CICB was performed every 3 d. (B) Proportion of 15 FMT donor feces (human responders [HR] and human nonresponders [HNR]) reflected in BALB/c mice (mice responders [MR] and mice nonresponders [MNR]), as described in Supplementary Table 4. Monitoring of RENCA progression using (C and E) bioluminescence imaging of luciferase activity or (C and D) tumor weight in ATB-treated mice after FMT with feces from five R and 10 NR RCC patients, treated with CICB and compensated by oral administration of commensals *A. muciniphila* (*Am*), *B. salyersiae* (*Bs*), or feces from R patients. All experiments involved five to seven mice per group (eg, colors in Fig. 3D) and were performed at least twice in similar conditions yielding similar results. ANOVA and Student *t* test statistical analyses of means ± SEM: * $p < 0.05$, ** $p < 0.01$, *** $p < 0.001$.

ANOVA = analysis of variance; ATB = antibiotic; CICB = combination immune checkpoint blocker; D0 = day of randomization; Dx = last IVIS measurement; mAb = monoclonal antibody; NR = nonresponder; PD-1 = programmed death 1; R = responder; RCC = renal cell carcinoma; RENCA = renal cell carcinoma; SEM = standard error of the mean.

representation of *A. senegalensis and A. muciniphila* induced by TKIs (LEfSe; Fig. 4A) was observed in these patients. Since we enrolled patients after failure of 1L (or more) TKIs, collection of feces preceding the introduction of TKIs was not available to uncouple the effects of tumor progression from that of TKIs on the microbiome shift. To circumvent this limitation, we administered in two different mouse genetic backgrounds a tumoricidal antiangiogenic dose of various TKIs (sunitinib, axitinib, or cabozantinib) over 3 wk and collected stools longitudinally. Strikingly, all three TKIs markedly induced significant changes in the alpha- and beta-diversity of the microbiota over time, in both BALB/c (Fig. 4B) and C57BL/6 mice, with a common dominant deviation of the microbiota composition (Supplementary Fig. 8). In BALB/c intestines, there was a prototypic TKI signature, with over-representation of *Eubacterium coprostanoligenes*, *Vampirovibrio chlorellavorus*, *Longibaculum muris*, *Parabacteroides goldsteinii*, *Alistipes timonensis,* and *Faecalicatena contorta*, with relatively lower dominance of *Neglecta timonensis*, *Adlercreutzia equolifaciens*, and *B. fragilis* 15 d after TKI uptake (mean VIP score). Importantly, sunitinib and cabozantinib favored a higher abundance of immunostimulatory *A. senegalensis*, as observed in humans (Fig. 4A and 4B). Accordingly, in C57BL/6 intestines, there was over-representation of the immunostimulatory *E. siraeum,* among other species shared by all three TKIs (Supplementary Fig. 8). Importantly, TKIs favored a higher abundance of immunostimulatory *A. senegalensis* and *A. muciniphila* (Fig. 4B), especially for cabozantinib. Overall, TKIs induced a significant and prototypic microbiota shift including immunostimulatory commensals that could be harnessed to improve the efficacy of ICBs in RCC patients.

4. Discussion

RCC encompasses a wide spectrum of morphologically and molecularly distinct cancer subtypes. The introduction of targeted therapies (inhibiting vascular endothelial growth factor [VEGF] receptor, platelet-derived growth factor, c-Met, and AXL) and ICBs into clinical practice has improved markedly the median OS in clear cell RCC patients, the most common subtype. With 12 approved drugs acting through

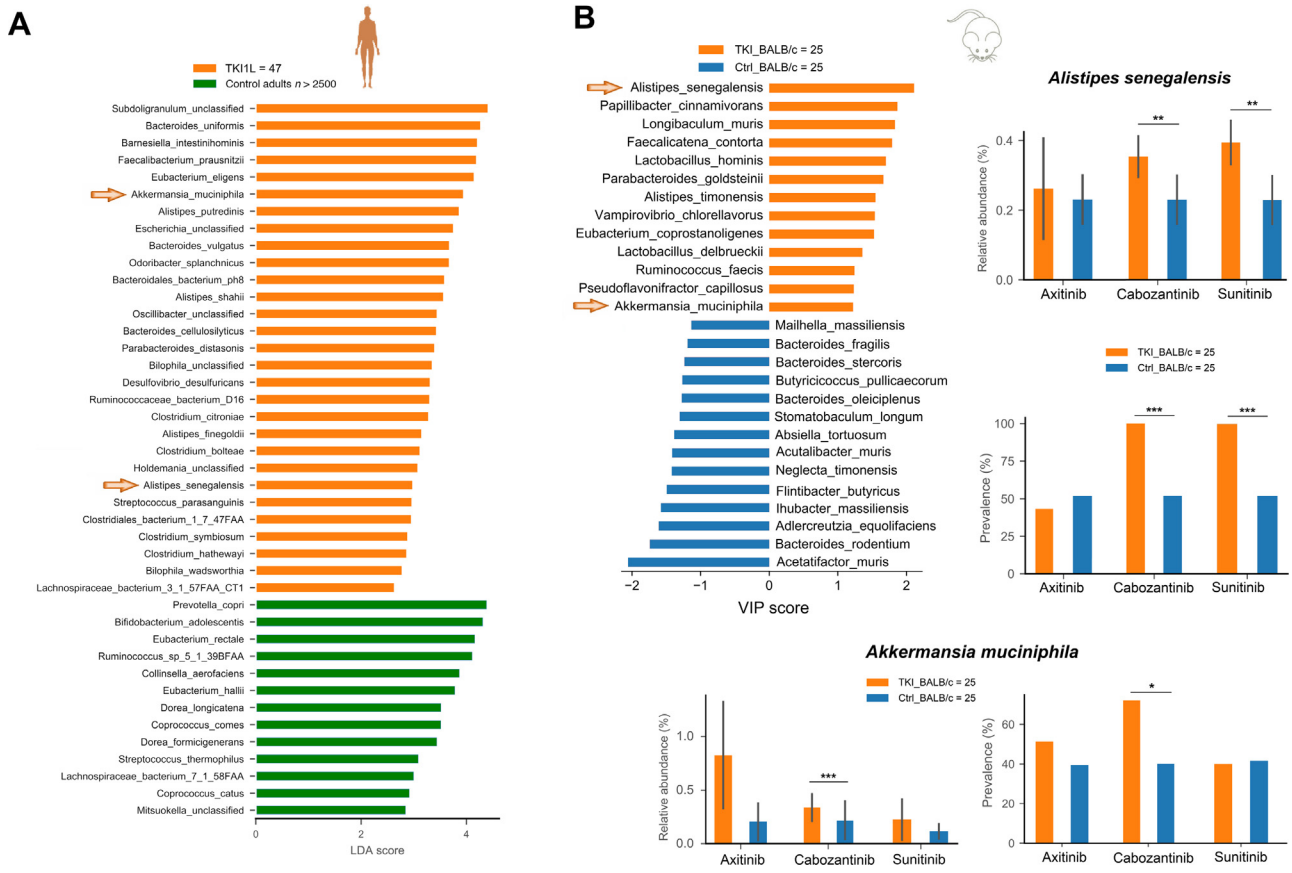

Fig. 4 – Fecal microbiota differences in patients and mice treated with TKI. Fecal microbiota compositional differences of (A) patients who underwent first-line TKI treatment and control adults, and (B) BALB/c mice that underwent TKI treatment (axitinib, sunitinib, and cabozantinib) were analyzed. Linear discriminant analysis of effect size and partial least square discriminant analysis coupled to variable importance plot (VIP) were implemented for humans and mice, respectively, in order to describe the most discriminant species in descending order of importance. In humans, we considered first-line TKI treatment (orange) compared with literature-based controls (green) (Fig. 4A), while in mice we considered the mean VIP score taken from the combined TKI. Briefly, VIP scores of all bacterial species that were present in at least two mice VIP plots were averaged and classified in descending order according to the species belonging to TKI (orange) or control (blue) cohort (Fig. 4B, arrows highlight relevant bacterial species). Relative abundance and prevalence of the most discriminant species for TKI group, *A. senegalensis*, and *A. muciniphila* were reported. For the three different TKIs (axitinib, sunitinib, and cabozantinib), a Mann-Whitney *U* test was used to assess statistical differences (* $p < 0.05$, ** $p < 0.01$, *** $p < 0.001$).

1L = first line; Ctrl = control; LDA = linear discriminant analysis; TKI = tyrosine kinase inhibitor.

six different effective mechanisms, novel biomarkers are needed to stratify and clarify this therapeutic landscape and improve efficacy safely. Based on pan-omics approaches integrating genetics, transcriptomics, immunoscoring, and molecular stratifications, we can in part stratify subgroups of patients with dismal prognosis that may benefit more specifically from antiangiogenic therapies or immunotherapies. However, it appears that some tumors are a desert of immune reactivities, while others are invaded with overt inflammatory and/or exhausted cell infiltrates that do not convey long-term protection, suggesting that the immune tone of RCC patients is not properly triggered or controlled.

Our study highlights the potential of harnessing the intestinal microbiome to better control the "cancer-immune set point" [39], that is, the threshold beyond which ICB triggers a clinical benefit. Mapping of the gut holobiont to identify a minimalist ecosystem governing the cancer-immune set point, and more specifically immunogenic versus tolerogenic commensals and medications tilting their balance, remains an open conundrum. By applying various bioinformatic and clinical subgroup analyses (LEfSe, PLS-DA, VIP, and networks), we identified a limited set of species (phylum Firmicutes, family Clostridiaceae, species *C. clostridioforme* and *C. hathewayi*) that were associated with primary resistance and enriched by ATB use and metastatic cancer status.

The "*C. clostridioforme* group" comprises three principal species that differ in virulence and antimicrobial susceptibility despite similar colony and microscopic morphology. *Clostridium bolteae* and *C. clostridioforme* are observed with approximately equal frequency, but *C. hathewayi* is seen with much greater frequency [40,41]. Infections with the "*C. clostridioforme* group" are the second most frequently isolated species of *Clostridium*, after *Clostridium perfringens* [40,41]. *C. hathewayi* has been reported to be a part of the pathobionts associated with the diagnosis of colon cancers [42] and could mitigate antigen-specific T-cell responses in mice [43].

Conversely, we identified some commensals associated with favorable prognosis and the intestinal homeostatic status, which belong to Eubacteriaceae (*E. rectale* and *E. siraeum*), Lachnospiraceae (*D. longicatena*), and Verrucomicrobioaceae (*A. muciniphila*) families and to the Bacteroidales order (Rikenellaceae family/Alistipes/*A. senegalensis,* Bacteroidaceae family/Bacteroides/*B. salyersiae*). While *A. senegalensis* and *A. muciniphila* alone or together within minimalist communities were clearly associated with the elicitation of adaptive immune responses beneficial against murine cancers [20,44], Eubacteriaceae and *D. longicatena* have been described as pivotal to keep in check the homeostasis of the intestinal barrier [45].

Experiments initially conducted in mice showed that broad-spectrum ATBs blunt the activity of ICBs against a wide range of transplantable and orthotopic tumors, suggesting that a minimalist intestinal ecosystem is required for the function of the mammalian host immune system [46]. These pioneering observations in preclinical models encouraged retrospective analyses in cancer patients to determine whether premedication with ATBs would influence the clinical response to ICBs. In the literature, retrospective analyses including >1800 patients assessed the impact of ATBs taken shortly before or after the initiation of ICBs on clinical outcome of patients treated with ICBs in several malignancies [47]. Eleven out of the 12 analyses reported a negative impact of ATB uptake on PFS and/or OS, mirroring the murine data [19–21]. However, the impact of these unexpected findings on the clinical management of cancer patients remains controversial. Here, we describe how ATBs (mostly beta-lactams and quinolones) affect the intestinal composition of feces of 69 RCC patients. ATBs markedly affected the beta-diversity, leading to the under-representation of Eubacteriaceae family members as already described [48] (such as *E. rectale)* for the benefit of pathobiont species (*E. bacterium_2_2_44A* and *C. hathewayi*). This microbiome shift is associated with a reduced ORR during ICB therapy (73% of primary resistance in the ATB vs 33% in the noATB subgroups, $p < 0.03$).

Given the incidence of gastrointestinal toxicity associated with TKIs, pioneering studies investigated TKI-induced dysbiosis and the impact of ATBs on diarrhea and survival. Pal et al [49] evaluated a population of 20 RCC patients receiving VEGF-TKIs, and reported a positive and a negative association between *Bacteroides* spp. or *Prevotella* spp. and diarrhea, respectively. When comparing the TKI-RCC stool data of the patients with those from HVs, they observed a relative loss of *Bifidobacterium* spp. Accordingly, Gong et al [50] followed up five RCC patients treated with TKIs and showed that *Bacteroides, Barnesiella*, and *Phascolarctobacterium* were elevated in Rs while *Bifidobacterium* was elevated in NRs. However, in parallel, Hahn et al [51] showed that ATBs targeting stool *Bacteroides* spp. improved PFS in patients receiving 1L VEGF-TKIs in a duration-dependent manner. Our data fuel this hypothesis of an unconventional mode of action of VEGF-TKIs, whereby a treatment-induced prototypic gut microbiome fingerprint might influence therapeutic outcome.

Limitations of our study include that this conclusion relies on a single cohort of 69 RCC patients including only 11 cases that took ATBs and in 2L therapy, with the interference of many confounding factors (prior therapies, comedications, and other factors such as hemoglobin [52,53]). Prospective studies in 1L therapy should validate this fingerprint as a new predictor of primary resistance to ICBs.

Some bacterial species appear to correlate with distinct hallmarks of activation and exhaustion of blood T lymphocytes, and to influence therapeutic outcome in the gut humanized avatar mouse models, implying that fecal microbiota composition may, to some extent, govern therapeutic outcome in patients. Analyses of stools before starting treatment thus have the potential to guide clinicians' decisions about eventually administering selected bacterial species or minimalist consortia for preventing primary resistance to immunotherapy in RCC patients. A better understanding of the mechanistic link between the microbial composition of the intestine and the local, systemic, and tumoral immune system will allow optimal design of compensatory therapies for gut dysbiosis in RCC cancer patients.

Author contributions: Lisa Derosa had full access to all the data in the study and takes responsibility for the integrity of the data and the accuracy of the data analysis.
Study concept and design: Derosa, Routy, Fidelle, Zitvogel.
Acquisition of data: Derosa.
Analysis and interpretation of data: Zitvogel, Derosa, Iebba, Escudier, Alla, Albiges.
Drafting of the manuscript: Zitvogel, Derosa.
Critical revision of the manuscript for important intellectual content: All authors.
Statistical analysis: Iebba, Alla, Albiges, Pasolli.
Obtaining funding: Zitvogel, Kroemer, Derosa, Routy.
Administrative, technical, or material support: Derosa.
Supervision: Zitvogel.
Other: None.

Financial disclosures: Lisa Derosa certifies that all conflicts of interest, including specific financial interests and relationships and affiliations relevant to the subject matter or materials discussed in the manuscript (eg, employment/affiliation, grants or funding, consultancies, honoraria, stock ownership or options, expert testimony, royalties, or patents filed, received, or pending), are the following: Laurence Zitvogel, Romain Daillère, and Guido Kroemer are cofounders of EverImmune, a biotech company devoted to the use of commensal microbes for the treatment of cancers. Laurence Zitvogel has a research contract with Kaleido and Innovate Pharma.

Funding/Support and role of the sponsor: Lisa Derosa was supported by the Philanthropia Foundation and ESMO translational research fellowship. Bertrand Routy was supported by the Philanthropia Foundation; Fonds de recherche en santé du Quebec and the Kidney Cancer Research Network of Canada. Laurence Zitvogel and Guido Kroemer were supported by the Ligue contre le Cancer (équipe labelisée); Agence National de la Recherche (ANR)— Projets blancs; ANR under the frame of E-Rare-2, the ERA-Net for Research on Rare Diseases; Association pour la recherche sur le cancer (ARC); Cancéropôle Ile-de-France; Chancelerie des universités de Paris (Legs Poix), Fondation de France; Fondation pour la Recherche Médicale (FRM); a donation by Elior; the European Commission (Horizon 2020: Oncobiome); the European Research Council (ERC); Fondation Carrefour; High-end Foreign Expert Program in China (GDW20171100085 and GDW20181100051), Institut National du Cancer (INCa); Inserm (HTE); Institut Universitaire de France; LeDucq Foundation; the LabEx Immuno-Oncology; the RHU Torino Lumière (ANR-16-RHUS-0008); the Searave and Carrefour Foundation; the SIRIC Stratified Oncology Cell DNA Repair and Tumor Immune Elimination (SOCRATE 2.0); ONCOBIOME H2020 network; the BMS Foundation; the SIRIC Cancer Research and Personalized Medicine (CARPEM); and the Paris Alliance of Cancer Research Institutes (PACRI). This work was supported by the French Government under the "Investissements d'avenir" (Investments for the Future) program managed by the Agence Nationale de la Recherche (ANR, fr: National Agency for Research; reference: Méditerranée Infection 10-IAHU-03), and by Région Provence Alpes Côte d'Azur and European funding FEDER PRIMI. The results shown here are based upon data generated by the TCGA Research Network (http://cancergenome.nih.gov/) and National Research, Development and Innovation Fund of Hungary (project no. FIEK_16-1-2016-0005). Z.S. was supported by the Research and Technology Innovation Fund NAP2-2017-1.2.1-NKP-0002, Breast Cancer Research Foundation (BCRF-17-156). Z.S and I.C. were supported by the Novo Nordisk Foundation Interdisciplinary Synergy Program Grant (NNF15OC0016584).

Acknowledgments: We are thankful to the animal facility team of Gustave Roussy and all the technicians from Centre GF Leclerc.

CRediT authorship contribution statement

Lisa Derosa: ConceptualizationData curation, Formal analysis, Funding acquisition, Investigation, Methodology, Project administration, Resources, Software, Supervision, Validation, Visualization, Writing - original draft. **Bertrand Routy**: Conceptualization, Data curation, Funding acquisition, Investigation, Methodology, Project administration, Validation. **Marine Fidelle**: ConceptualizationValidation. **Valerio Iebba**: Formal analysisMethodology, Validation, Visualization. **Laurie Alla**: Validation. **Edoardo Pasolli**: Validation. **Nicola Segata**: Validation. **Aude Desnoyer**: Validation. **Filippo Pietrantonio**: Validation. **Gladys Ferrere**: Validation. **Jean-Eudes Fahrner**: Validation. **Emmanuelle Le Chatellier**: Validation. **Nicolas Pons**: Validation. **Nathalie Galleron**: Validation. **Hugo Roume**: Validation. **Connie P.M. Duong**: Validation. **Laura Mondragón**: Validation. **Kristina Iribarren**: Validation. **Mélodie Bonvalet**: Validation. **Safae Terrisse**: Validation. **Conrad Rauber**: Validation. **Anne-Gaëlle Goubet**: Validation. **Romain Daillère**: Validation. **Fabien Lemaitre**: Validation. **Anna Reni**: Validation. **Beatrice Casu**: Validation. **Maryam Tidjani Alou**: Validation. **Carolina Alves Costa Silva**: Validation. **Didier Raoult**: Validation. **Karim Fizazi**: Validation. **Bernard Escudier**: Validation. **Guido Kroemer**: Validation. **Laurence Albiges**: Validation. **Laurence Zitvogel**: ConceptualizationFunding acquisition, Investigation, Methodology, Validation, Writing - original draft.

References

[1] Escudier B, Farace F, Angevin E, et al. Immunotherapy with interleukin-2 (IL2) and lymphokine-activated natural killer cells: improvement of clinical responses in metastatic renal cell carcinoma patients previously treated with IL2. Eur J Cancer 1994;30A:1078–83.
[2] Motzer RJ, Hutson TE, Tomczak P, et al. Sunitinib versus interferon alfa in metastatic renal-cell carcinoma. N Engl J Med 2007;356:115–24.
[3] Rosenberg SA, Lotze MT, Yang JC, et al. Prospective randomized trial of high-dose interleukin-2 alone or in conjunction with lymphokine-activated killer cells for the treatment of patients with advanced cancer. J Natl Cancer Inst 1993;85:622–32.
[4] Becht E, Giraldo NA, Beuselinck B, et al. Prognostic and theranostic impact of molecular subtypes and immune classifications in renal cell cancer (RCC) and colorectal cancer (CRC). Oncoimmunology 2015;4:e1049804.
[5] Becht E, Giraldo NA, Lacroix L, et al. Estimating the population abundance of tissue-infiltrating immune and stromal cell populations using gene expression. Genome Biol 2016;17:218.
[6] Chevrier S, Levine JH, Zanotelli VRT, et al. An immune atlas of clear cell renal cell carcinoma. Cell 2017;169, 736–49.e18.
[7] Ascierto ML, McMiller TL, Berger AE, et al. The intratumoral balance between metabolic and immunologic gene expression is associated

with anti–PD-1 response in patients with renal cell carcinoma. Cancer Immunol Res 2016;4:726–33.
[8] Giraldo NA, Becht E, Pagès F, et al. Orchestration and prognostic significance of immune checkpoints in the microenvironment of primary and metastatic renal cell cancer. Clin Cancer Res 2015;21:3031–40.
[9] Giraldo NA, Becht E, Vano Y, et al. Tumor-infiltrating and peripheral blood t-cell immunophenotypes predict early relapse in localized clear cell renal cell carcinoma. Clin Cancer Res 2017;23:4416–28.
[10] Motzer RJ, Escudier B, McDermott DF, et al. Nivolumab versus everolimus in advanced renal-cell carcinoma. N Engl J Med 2015;373:1803–13.
[11] Motzer RJ, Tannir NM, McDermott DF, et al. Nivolumab plus ipilimumab versus sunitinib in advanced renal-cell carcinoma. N Engl J Med 2018;378:1277–90.
[12] Porta C, Rizzo M. Immune-based combination therapy for metastatic kidney cancer. Nat Rev Nephrol 2019;15:324–5.
[13] Rini BI, Plimack ER, Stus V, et al. Pembrolizumab plus axitinib versus sunitinib for advanced renal-cell carcinoma. N Engl J Med 2019;380:1116–27.
[14] Rini BI, Powles T, Atkins MB, et al. Atezolizumab plus bevacizumab versus sunitinib in patients with previously untreated metastatic renal cell carcinoma (IMmotion151): a multicentre, open-label, phase 3, randomised controlled trial. Lancet 2019;393:2404–15.
[15] Motzer RJ, Penkov K, Haanen J, et al. Avelumab plus axitinib versus sunitinib for advanced renal-cell carcinoma. N Engl J Med 2019;380:1103–15.
[16] Casuscelli J, Vano Y-A, Fridman WH, Hsieh JJ. Molecular classification of renal cell carcinoma and its implication in future clinical practice. Kidney Cancer 2017;1:3–13.
[17] Beuselinck B, Job S, Becht E, et al. Molecular subtypes of clear cell renal cell carcinoma are associated with sunitinib response in the metastatic setting. Clin Cancer Res 2015;21:1329–39.
[18] Kroemer G, Zitvogel L. Cancer immunotherapy in 2017: the breakthrough of the microbiota. Nat Rev Immunol 2018;18:87–8.
[19] Derosa L, Hellmann MD, Spaziano M, et al. Negative association of antibiotics on clinical activity of immune checkpoint inhibitors in patients with advanced renal cell and non-small-cell lung cancer. Ann Oncol 2018;29:1437–44.
[20] Routy B, Le Chatelier E, Derosa L, et al. Gut microbiome influences efficacy of PD-1-based immunotherapy against epithelial tumors. Science 2018;359:91–7.
[21] Elkrief A, El Raichani L, Richard C, et al. Antibiotics are associated with decreased progression-free survival of advanced melanoma patients treated with immune checkpoint inhibitors. Oncoimmunology 2019;8:e1568812.
[22] Gopalakrishnan V, Spencer CN, Nezi L, et al. Gut microbiome modulates response to anti-PD-1 immunotherapy in melanoma patients. Science 2018;359:97–103.
[23] Matson V, Fessler J, Bao R, et al. The commensal microbiome is associated with anti-PD-1 efficacy in metastatic melanoma patients. Science 2018;359:104–8.
[24] Sivan A, Corrales L, Hubert N, et al. Commensal *Bifidobacterium* promotes antitumor immunity and facilitates anti-PD-L1 efficacy. Science 2015;350:1084–9.
[25] Vétizou M, Pitt JM, Daillère R, et al. Anticancer immunotherapy by CTLA-4 blockade relies on the gut microbiota. Science 2015;350:1079–84.
[26] Daillère R, Vétizou M, Waldschmitt N, et al. *Enterococcus hirae* and *Barnesiella intestinihominis* facilitate cyclophosphamide-induced therapeutic immunomodulatory effects. Immunity 2016;45:931–43.
[27] Routy B, Gopalakrishnan V, Daillère R, Zitvogel L, Wargo JA, Kroemer G. The gut microbiota influences anticancer immunosurveillance and general health. Nat Rev Clin Oncol 2018;15:382–96.
[28] Assel M, Sjoberg D, Elders A, et al. Guidelines for reporting of statistics for clinical research in urology. BJU Int 2019;123:401–10.
[29] Albiges L, Negrier S, Dalban C, et al. Safety and efficacy of nivolumab in metastatic renal cell carcinoma (mRCC): results from the NIVOREN GETUG-AFU 26 study. J Clin Oncol 2018;36:577.
[30] Eisenhauer EA, Therasse P, Bogaerts J, et al. New response evaluation criteria in solid tumours: revised RECIST guideline (version 1.1). Eur J Cancer 1990 2009;45:228–47.
[31] European Commission. Final report summary—IHMS (International Human Microbiome Standards) | Report summary | IHMS | FP7 | CORDIS. https://cordis.europa.eu/project/id/261376/reporting.
[32] Li J, Jia H, Cai X, et al. An integrated catalog of reference genes in the human gut microbiome. Nat Biotechnol 2014;32:834–41.
[33] Nielsen HB, Almeida M, Juncker AS, et al. Identification and assembly of genomes and genetic elements in complex metagenomic samples without using reference genomes. Nat Biotechnol 2014;32:822–8.
[34] Segata N, Waldron L, Ballarini A, Narasimhan V, Jousson O, Huttenhower C. Metagenomic microbial community profiling using unique clade-specific marker genes. Nat Methods 2012;9:811–4.
[35] Li M, Wang B, Zhang M, et al. Symbiotic gut microbes modulate human metabolic phenotypes. Proc Natl Acad Sci 2008;105:2117–22.
[36] Segata N, Izard J, Waldron L, et al. Metagenomic biomarker discovery and explanation. Genome Biol 2011;12:R60.
[37] *Hungatella hathewayi* | Semantic Scholar. https://www.semanticscholar.org/topic/Hungatella-hathewayi/1069858.
[38] Zhao L, Zhang F, Ding X, et al. Gut bacteria selectively promoted by dietary fibers alleviate type 2 diabetes. Science 2018;359:1151–6.
[39] Chen DS, Mellman I. Elements of cancer immunity and the cancer-immune set point. Nature 2017;541:321–30.
[40] Dababneh AS, Nagpal A, Palraj BRV, Sohail MR. *Clostridium hathewayi* bacteraemia and surgical site infection after uterine myomectomy. BMJ Case Rep 2014;2014:bcr2013009322.
[41] Finegold SM, Song Y, Liu C, et al. *Clostridium clostridioforme*: a mixture of three clinically important species. Eur J Clin Microbiol Infect Dis 2005;24:319–24.
[42] Liang Q, Chiu J, Chen Y, et al. Fecal bacteria act as novel biomarkers for noninvasive diagnosis of colorectal cancer. Clin Cancer Res 2017;23:2061–70.
[43] Rossi O, van Berkel LA, Chain F, et al. *Faecalibacterium prausnitzii* A2-165 has a high capacity to induce IL-10 in human and murine dendritic cells and modulates T cell responses. Sci Rep 2016;6:18507.
[44] Tanoue T, Morita S, Plichta DR, et al. A defined commensal consortium elicits CD8 T cells and anti-cancer immunity. Nature 2019;565:600.
[45] Kamo T, Akazawa H, Suda W, et al. Dysbiosis and compositional alterations with aging in the gut microbiota of patients with heart failure. PLoS One 2017;12:e0174099.
[46] Clavel T, Gomes-Neto JC, Lagkouvardos I, Ramer-Tait AE. Deciphering interactions between the gut microbiota and the immune system via microbial cultivation and minimal microbiomes. Immunol Rev 2017;279:8–22.
[47] Elkrief A, Derosa L, Kroemer G, Zitvogel L, Routy B. The negative impact of antibiotics on outcomes in cancer patients treated with immunotherapy: a new independent prognostic factor? Ann Oncol Off J 2019;30:1572–9.
[48] Raymond F, Ouameur AA, Déraspe M, et al. The initial state of the human gut microbiome determines its reshaping by antibiotics. ISME J 2016;10:707–20.
[49] Pal SK, Li SM, Wu X, et al. Stool bacteriomic profiling in patients with metastatic renal cell carcinoma receiving vascular endothelial growth factor-tyrosine kinase inhibitors. Clin Cancer Res 2015;21:5286–93.

[50] Gong J, Noel S, Pluznick JL, Hamad ARA, Rabb H. Gut microbiota-kidney cross-talk in acute kidney injury. Semin Nephrol 2019;39:107–16.

[51] Hahn AW, Froerer C, VanAlstine S, et al. Targeting *Bacteroides* in stool microbiome and response to treatment with first-line VEGF tyrosine kinase inhibitors in metastatic renal-cell carcinoma. Clin Genitourin Cancer 2018;16:365–8.

[52] Maier L, Pruteanu M, Kuhn M, et al. Extensive impact of non-antibiotic drugs on human gut bacteria. Nature 2018;555: 623–8.

[53] Pasolli E, Asnicar F, Manara S, et al. Extensive unexplored human microbiome diversity revealed by over 150,000 genomes from metagenomes spanning age, geography, and lifestyle. Cell 2019;176, 649–62.e20.